J. Physiol. (1983), **345**, *pp.* 353–372
With 11 *text-figures*
Printed in Great Britain

VOLTAGE-CLAMP STUDY OF THE CONDUCTANCE ACTIVATED AT FERTILIZATION IN THE STARFISH EGG

BY JEFFRY B. LANSMAN

From the Department of Physiology, Jerry Lewis Neuromuscular Research Center, and Ahmanson Laboratory of the Brain Research Institute, School of Medicine, University of California, Los Angeles, CA 90024, U.S.A.

(*Received 13 January 1983*)

SUMMARY

1. Ionic currents underlying the fertilization potential of the egg of the starfish *Mediaster aequalis* were studied using a two-micro-electrode voltage clamp.

2. Mature eggs were fertilized *in vitro* under voltage-clamp conditions. The fertilization current, here termed I_F, was induced by adding sperm to sea water bathing the egg. At a holding potential of −70 mV, I_F was inward. It reached a peak within 2–4 min and then decayed over the next approximately 20 min with a rate which depended on the holding membrane potential.

3. Instantaneous current–voltage relations measured at different times during I_F were approximately linear and reversed at a potential of $+6{\cdot}0 \pm 5{\cdot}8$ mV (mean ± S.D., $n = 11$).

4. Membrane chord conductance was highest at the peak of inward current and the declining phase of I_F was due to a decrease in conductance towards the pre-fertilization level.

5. When the membrane potential was rapidly stepped to levels more positive than about −45 mV, the conductance underlying I_F decreased in a manner which depended on both membrane potential and time.

6. The fertilization-specific conductance showed a sigmoidal activation curve between −50 and +10 mV with a half-activation level of −25 mV. Analysis of the steady-state voltage dependence indicated that at the peak of the fertilization potential (+10 to +15 mV) only 4–5% of the total available channels would be open.

7. Current relaxations followed first-order kinetics and the relaxation time constant depended upon the membrane potential during the voltage pulse. The relation between the time constant and voltage was bell-shaped, decreasing at potentials more negative than −40 and more positive than 0 mV.

8. Both the steady-state conductance–voltage relation and the kinetics of the current relaxations were consistent with a simple two-state gating model in which the probability of a channel being open is determined by a single gating particle with an effective valency of −1·7 moving through the entire membrane field.

9. The shifts in reversal potential with changes in external Na (at 10 mM-external K) were analysed using the constant field expression, which gave a relative permeability of Na to K of approximately 0·6.

10. Comparison of reversal potentials for I_F measured in sea water in which Na was replaced with Li, Cs or Rb, yielded the permeability sequence Rb > K > Cs,Na > Li.

11. The results show that in the starfish egg the process of fertilization induces a relatively non-selective increase in cation permeability which is controlled by both fast and slow voltage-dependent processes.

INTRODUCTION

The attachment of a single spermatozoon to the egg membrane during fertilization initiates a transient electrical excitation, the fertilization potential, which appears to be one of the earliest detectable responses of egg to sperm. Potential changes at fertilization have been described in the eggs of polychaetes, echinoderms, amphibians, fish, ascidians and mammals (for review see Hagiwara & Jaffe, 1979).

In the echinoderm egg the initial interaction of sperm and egg results in a depolarization of the egg membrane which, after triggering an action potential, shifts to a positive level for many minutes (Jaffe, 1976; Chambers & DiArmendi, 1979; Miyazaki, 1979). The slower, sperm-dependent depolarization is due to the entry of Na ions (Steinhardt, Lundin & Mazia, 1971; Ito & Yoshioka, 1973; Chambers & DiArmendi, 1979) and is associated with an increase in total conductance of the egg membrane (McClendon, 1910; Hiramoto, 1959; Ito & Yoshioka, 1973; Miyazaki, Ohmori & Sasaki, 1975*b*). How the interaction of the gamete membranes triggers the permeability change is not known. Basic information on the time course, sensitivity to membrane potential, and ion dependence of fertilization-generated currents is required in order to draw general conclusions about the mechanism of the underlying permeability changes. With this information we may then ask how the electrical events at fertilization are related to the general programme of activation and early embryogenesis of the egg.

This paper reports a study of the membrane currents activated by sperm during *in vitro* fertilization of eggs of the starfish, *Mediaster aequalis*. Several properties of the permeability change underlying the fertilization potential are described and their relation to cellular events occurring during fertilization considered.

METHODS

Preparation

Ripe specimens of the starfish, *Mediaster aequalis*, were obtained during the months of January to April. Animals were maintained in an artificial sea-water aquarium (Instant Ocean Systems) at 9–11 °C. In order to obtain immature oocytes, ovaries were dissected from females, rinsed once in Ca-free seawater, and incubated for about 1 h in this solution. This procedure induces spawning while preventing spontaneous maturation (Ikegami, 1976). Upon returning the ovaries to sea water containing Ca, a number of immature ooytes were released. These were immobilized in the bottom of a Plexiglas chamber with a cage made of small steel pins. Solution was continually perfused through an ice bath. All experiments were done at 15–17 °C.

Electrical recording and voltage clamp

Cells were impaled with two micro-electrodes filled with 3 M-KCl (resistance $1–5 \times 10^6\ \Omega$). Membrane potential was recorded differentially between one intracellular micro-electrode and a third KCl-filled micro-electrode in the bath. Cells were voltage clamped using a conventional circuit. In a typical cell the capacitive transient settled within 2 ms. Current was measured as the voltage drop across a $1 \times 10^6\ \Omega$ resistor in the feed-back loop of an operational amplifier which held the bath

at virtual ground through an agar–seawater bridge. The resistance in series with the voltage electrode was small (less than 2 KΩ) and no compensation was used.

Solutions

All experiments were done in artificial sea water (ASW) which contained 470 mM-NaCl, 10 mM-KCl, 50 mM-$MgCl_2$, 10 mM-$CaCl_2$, and was buffered with 2·4 mM-$NaHCO_3$ and 10 mM-HEPES to pH 7·8. When Ca was changed, the $MgCl_2$ concentration was altered so as to maintain a constant concentration of divalent cations. For experiments involving Na substitution, Na was replaced with choline. Li, Cs or Rb ASW was made by substituting the appropriate cation for Na at equimolar concentration. The hormone 1-methyladenine (1-MA) was stored frozen as a 3 mM stock solution in distilled water and, before use, was diluted to a final concentration of 50 μM in ASW

In vitro maturation and fertilization

After an immature oocyte had been impaled with two micro-electrodes, the perfusing solution was switched to ASW containing 50 μM-1-MA. Exposure to this hormone releases the immature oocyte from developmental arrest at meiotic prophase and induces the subsequent breakdown of the germinal vesicle and formation of polar bodies (Kanatani, 1973). The germinal vesicle in immature *Mediaster* oocytes appeared as a bright translucent spot about 50 μm in diameter near the oocyte surface. When oriented properly in the experimental chamber, it could be watched during the course of an experiment. Germinal vesicle breakdown in *Mediaster* required about 2–3 h to reach completion. Associated with germinal vesicle breakdown was a change in membrane input resistance which began some 30–40 min after exposure to 1-MA (Miyazaki *et al.* 1975*b*; Shen & Steinhardt, 1976). Cells showing this early electrical sign of maturation were fertilized.

Sperm suspension was freshly prepared by dissecting a small piece of testis from a male starfish and shaking it in 10 ml of ASW containing 0·1 mM-histidine. A 10–25 μl aliquot of this suspension was added to the experimental chamber. Fertilization membranes elevated about 20 min after insemination, although in many cases did not become conspicuous until some 1–2 h after insemination. This may be due to variability in the rate and extent of the cortical reaction.

RESULTS

Fertilization potential

Membrane potential changes associated with the induction of meiotic maturation by the hormone 1-MA, and the subsequent activation of the mature egg by sperm, are shown in Fig. 1. An immature oocyte was exposed to 1-MA and hyperpolarizing current pulses applied to the membrane. Within 30 min after exposure to hormone the input resistance increased due to a decrease in the inwardly rectifying K conductance, as reported in other starfish eggs (Miyazaki *et al.* 1975*b*; Shen & Steinhardt, 1976; Moody & Lansman, 1983). Both before and after maturation, Ca-dependent action potentials could be elicited with depolarizing current pulses (Miyazaki *et al.* 1975*a*; Hagiwara, Ozawa & Sand, 1975; Shen & Steinhardt, 1976). When a drop of sperm suspension was added to the chamber, the egg depolarized triggering an action potential. The membrane potential slowly depolarized again and reached a plateau level of between +10 and +15 mV where it remained for about 10 min before repolarizing. Periodic voltage oscillations were commonly seen at the plateau level of the fertilization potential. The time course of repolarization varied from egg to egg, and many eggs failed to repolarize at all. With careful impalements using a single micro-electrode, the potential returned to rest in about 30 min. Failure of the egg to repolarize completely during an experiment may have been due to electrode damage during the cortical reaction. In the experiment shown in Fig. 1, the fertilization membrane appeared about 20 min after insemination. It was characteristically low (100 μm), irregular, and failed to elevate over the entire egg.

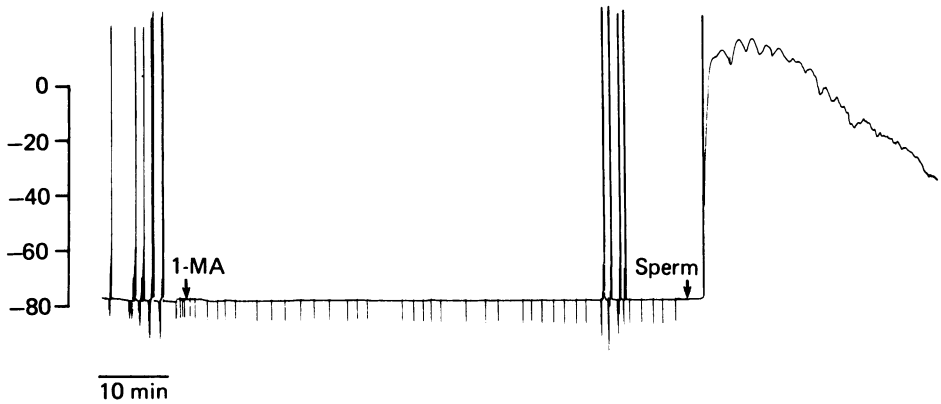

Fig. 1. Fertilization potential of *Mediaster aequalis* egg. The egg was first matured *in vitro* with 1-methyladenine (1-MA). After exposure to the hormone for 1 h sperm was added, producing the characteristic potential response.

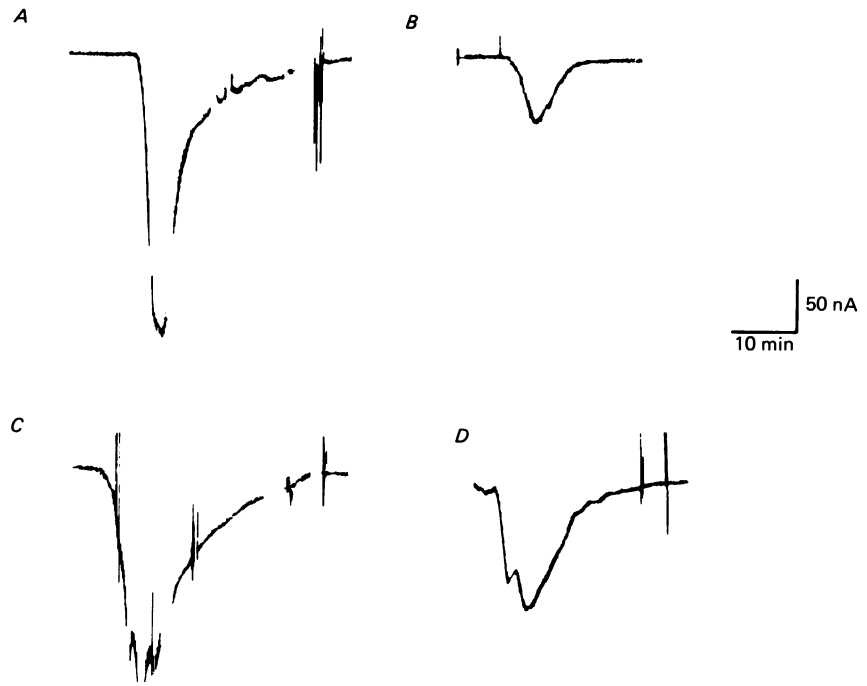

Fig. 2. Fertilization currents measured under voltage clamp in four different eggs. Holding potentials were −30 mV in *A* and *B* and −70 mV in *C* and *D*. Inward current is down. The chart-recorder pen was lifted from the paper at the interruptions in the record, which indicate when pulses were applied to the membrane.

Membrane current under voltage clamp

To observe the time course of membrane current flowing during the fertilization potential, the membrane potential of an egg was held at either −70 or −30 mV during fertilization, as shown in Fig. 2. The records in Fig. 2 show the fertilization current of eggs from four different females. The fertilization current, I_F, turned on and then

decayed following a time course roughly similar to the potential change. The amplitude of I_F varied considerably in different batches of eggs. Two factors may have contributed to this variability. The maximum amplitude of I_F depended on the concentration of sperm added, although this point was not systematically studied. In starfish eggs polyspermy is frequently associated with egg membrane potentials less than 0 mV (Miyazaki & Hirai, 1981), suggesting that there may have been a high incidence of polyspermy in eggs clamped at negative potentials. In eggs of the marine worm *Urechis* uptake of ^{24}Na is proportional to the number of sperm entering during experimentally induced polyspermy (Jaffe, Gould-Somero & Holland, 1979). The size of I_F in the starfish egg may, therefore, reflect the degree of polyspermy. A second factor was a declining receptivity of egg for sperm suggested by the observation that I_F became smaller towards the end of the breeding season. Both factors may have contributed to the size variability.

Fig. 2 also illustrates the effect of the holding potential on the time course of I_F. Current decayed more rapidly when the egg membrane was clamped at -30 mV than at -70 mV. Since the falling phase was not a simple exponential, this point was analysed by comparing the half-decay times ($t_{\frac{1}{2}}$) of I_F. At a holding potential of -30 mV, $t_{\frac{1}{2}}$ was 2·4 min (Fig. 2*A*) and 3·2 min (Fig. 2*B*), while at -70 mV, $t_{\frac{1}{2}}$ was 4·8 min (Fig. 2*C*) and 6·0 min (Fig. 2*D*). Furthermore, comparison of records 2*A* and 2*D* or 2*B* and 2*C* indicates that $t_{\frac{1}{2}}$ does not depend on the size of I_F. This is interpreted to indicate that a voltage-sensitive process controls the over-all time course of I_F.

Conductance change during fertilization

The starfish egg membrane possesses several time- and voltage-dependent ion channels underlying action potential generation. The relation of currents responsible for the action potential to I_F was examined by comparing the responses of the egg membrane to voltage steps before fertilization, to those recorded at various times during I_F. Fig. 3 shows the results from such an experiment.

In the mature egg before fertilization, the leak conductance was minimal as judged by the lack of an ohmic current displacement in response to a voltage step. During fertilization, the current required to hold the membrane potential at the resting level became inward. At 8 min after insemination it reached -320×10^{-9} A. When a voltage pulse was applied to the membrane, the current was displaced instantaneously from the steady level. The jump in current shows the increase in membrane chord conductance associated with fertilization. The change in the conductance of the egg membrane at the resting potential can be seen by comparing the first row of current records in Fig. 3*A*.

The changes in conductance of the egg membrane during fertilization were examined by plotting the instantaneous currents (measured 10 ms after the onset of the pulse) as a function of the potential during the step. Instantaneous current–voltage (I–V) relations were measured at 8 min after insemination when I_F reached its peak inward level (open triangles, Fig. 3*B*) and at 17 min after insemination when the steady current had declined to -100×19^{-9} A (open squares, Fig. 3*B*). The instantaneous currents depended linearly on membrane potential and the I–V relations intersected at a reversal potential of approximately +8 mV (Fig. 3*B*). Reversal potentials did not change significantly with time. The maximum error in

determining the reversal potential by extrapolating the instantaneous I–V relations to zero current was ±5 mV, so that smaller actual changes in reversal potential could not be resolved. Fig. 3*B* shows that the conductance of the egg membrane reached a maximum at the peak of I_F and then declined, indicating that the falling phase of I_F was not due to the development of an outward counter-current. Therefore, the time course of I_F reflects a time-dependent change in membrane conductance.

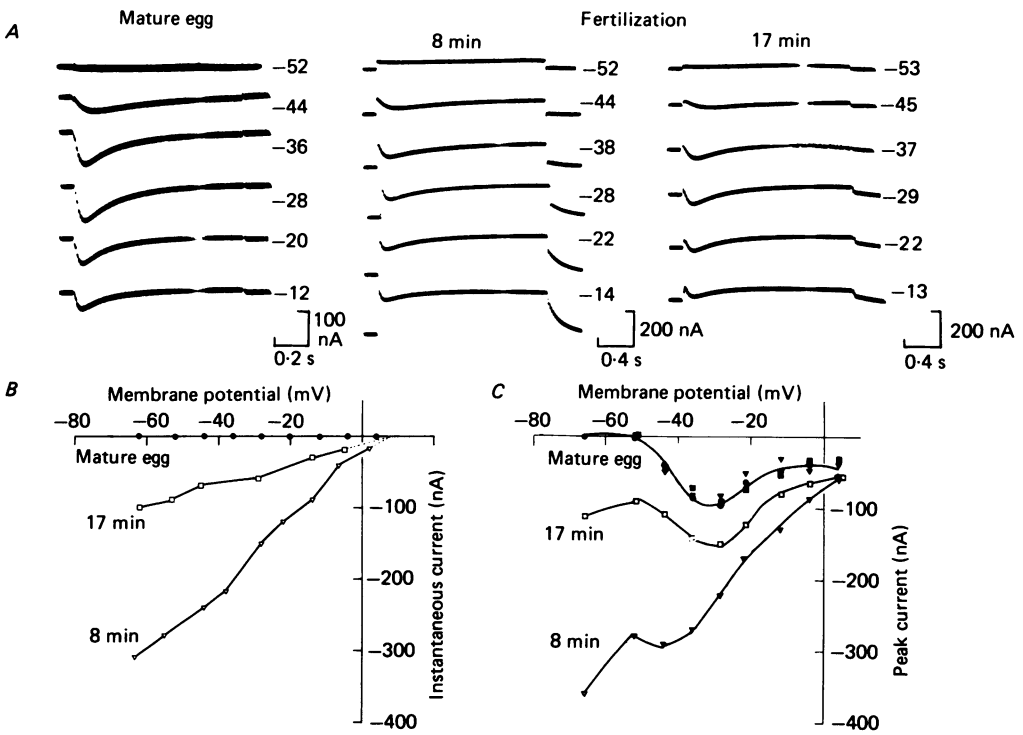

Fig. 3. Response of the egg membrane to voltage steps before and during fertilization. Sperm was added at zero time and I–V relations measured 8 and 17 min later. The holding potential was −62 mV. At 8 min a steady inward current of -330×10^{-9} A was flowing and the voltage-clamp records represent displacements from this level. At 17 min the steady current had declined to aproximately -100×10^{9} A. In *B* the instantaneous current (measured 10 ms after the onset of the pulse) is plotted as a function of potential (filled circles, unfertilized egg; open triangles, 8 min after insemination; open squares, 17 min after insemination). In *C* the peak of the transient inward current (measured from the zero current level) is plotted as a function of membrane potential (filled circles, unfertilized egg; open triangles, 8 min after insemination; open squares, 17 min after insemination). In *C* subtraction of the instantaneous current from the peak current is indicated by the filled triangles (8 min) and filled squares (17 min).

The relation of the Ca current to the total membrane current evoked by voltage steps during fertilization is shown in Fig. 3*C*. Before fertilization (Fig. 1*A*, column 1), voltage steps to potentials more positive than −50 mV activate an inward Ca current (Hagiwara *et al.* 1975). This current turns on from the zero current level and inactivates completely by the end of a 1 s voltage pulse. Filled circles in Fig. 3*C* plot peak inward Ca current as a function of voltage in the unfertilized egg. There are

two regions of negative slope corresponding to the two distinct Ca currents in the starfish egg membrane (Hagiwara *et al.* 1975). Ca currents are also seen in the fertilization records (note scale change for records at 8 and 17 min, Fig. 3*A*) but appear displaced from the base line current. The peak inward Ca current (measured from the zero current level) is plotted as a function of potential for currents evoked at 8 min (open triangles, Fig. 3*C*) and 17 min (open squares, Fig. 3*C*) as before. These *I–V* relations appear similar in form to the peak Ca current *I–V* relation in the unfertilized egg, but shifted by the addition of a linear component. Subtraction of the instantaneous current obtained from Fig. 3*B* from the peak current shown in Fig. 3*C* for each voltage yielded the filled symbols in Fig. 3*C*. This subtraction procedure, which is not much different from a linear leak subtraction, regenerates the original *I–V* relations of the unfertilized egg, which confirms that the separation procedure is adequate. Furthermore, neither the magnitude nor the activation voltage of the Ca current changed during the time course of I_F.

Steady-state voltage dependence

The experiments described in this section examined the steady-state voltage dependence of I_F. The first piece of evidence suggesting that the conductance underlying I_F could be turned rapidly on and off by voltage changes was the appearance during fertilization of a tail current when the membrane potential was repolarized to the holding potential following a voltage step (see records for 8 min in Fig. 3*A*, −38 to −14 mV). Experiments described below demonstrate that during depolarizing voltage steps I_F turns off and the tail current represents a conductance relaxation back to the level appropriate to the holding potential.

The turn-off of I_F by depolarizing voltages and the recovery after the termination of the pulse are shown in Fig. 4*A*. The current records were made by stepping the membrane potential from rest in 10 mV steps during the peak of I_F (note zero current level in this record) and superimposing the traces on the oscilloscope. The instantaneous currents behaved in a simple ohmic manner. At potentials more positive than about −45 mV, outwardly directed tail currents appeared after terminating the voltage step. At these potentials the ohmic jump in current at the end of the pulse was smaller than the current jump at the beginning of the pulse. Since the voltage displacements were identical, the conductance had decreased during the pulse.

These relaxations are analysed (see inset in Fig. 4*A*) by assuming that the change in current immediately before and after a rapid change in potential is due only to the change in driving force for ionic current flow. It is assumed that the number of open channels has not had time to change. Furthermore, currents due to either leak or Ca permeability are negligible at the beginning and end of the voltage step. If n_0 is the number of channels open at the beginning of the voltage pulse and n_∞ is the number of channels open at the end of the pulse, then

$$\begin{aligned} I_s &= n_0 i', \\ I_0(V) &= n_0 i'', \\ I_s(V) &= n_\infty i'', \\ I_0 &= n_\infty i', \end{aligned}$$

where I_s is the steady current at the holding potential, $I_0(V)$ is the instantaneous current at the test potential (V), $I_s(V)$ is the steady-state current at the end of the

test potential, I_0 is the instantaneous current after repolarizing the membrane to the holding potential, and i' and i'' are the single channel currents at the holding and test potentials, respectively. Then taking the ratio of the instantaneous jumps:

$$\frac{I_0 - I_s(V)}{I_s - I_0(V)} = \frac{n_\infty}{n_0}$$

gives the fraction of open channels. This parameter is equivalent to a normalized conductance. It is plotted in Fig. 4*B* as a function of membrane potential. The analysis shows that once open, channels can be induced to close by depolarizing the membrane from the resting potential. Fig. 4*B* predicts that at the peak of the fertilization potential only about 4% of the available channels would be open.

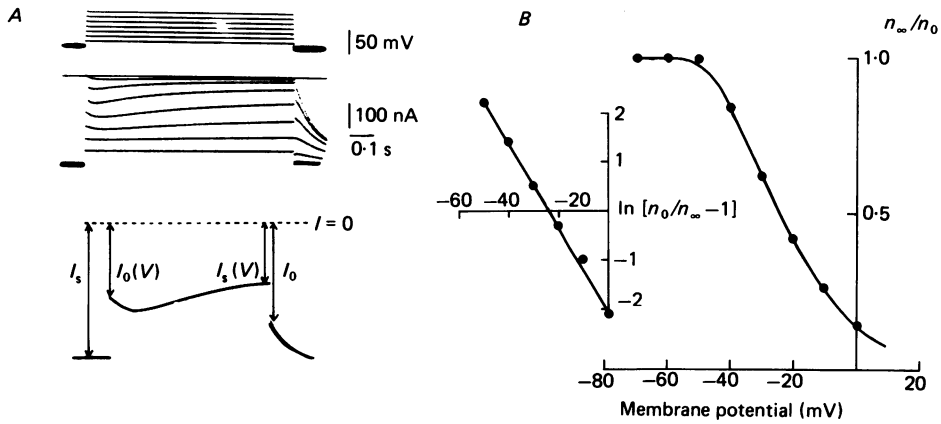

Fig. 4. Steady-state voltage dependence of the fertilization current. *A* shows the response of the egg to voltage steps during fertilization. Traces were superimposed on the oscilloscope. Line above current record indicates zero current level. Holding potential was −70 mV. Inset shows how current relaxations were measured. The Ca current relaxations were very small so that the voltage-dependent relaxations of the fertilization current are more prominent. In *B* the ratio of the instantaneous jumps at the end and the beginning of the voltage pulse, I_0–I_S $(V)/I_s$–I_0 (V), is plotted as a function of membrane potential. This parameter is equivalent to n_∞/n_0, the fraction of open channels (see text).

The steady-state analysis suggests that, once activated, the conductance underlying I_F can be controlled by voltage. When the membrane potential reaches a new level, the number of open channels reaches a value appropriate to the new potential. According to this view, all voltage dependence resides in the gating of I_F. This view is supported by the results of a previous section (Fig. 3*B*) which showed a linear instantaneous *I–V* relation. In this section, voltage-dependent gating of I_F is analysed by comparing the experimental results with the predictions of a simple kinetic model.

Channel opening and closing are assumed to be controlled by a gating charge which must traverse a single energy barrier, with the steady-state distribution of gating charge determining the number of conducting channels in the whole cell. This model requires only that the rate constants governing the movement of the gating particle

depend exponentially on membrane potential. If the transition between conducting and non-conducting states follows a unimolecular reaction:

$$a \underset{\beta}{\overset{\alpha}{\rightleftharpoons}} b$$

and

$$\alpha = f\exp[\delta m V^* F/RT]; \quad \beta = f\exp -[(1-\delta)\, m V^* F/RT],$$

where f is a frequency factor close to or less than kT/h in units of s^{-1}; m is proportional to the steepness of the function; V^* is $V-V_{\frac{1}{2}}$ where V is membrane potential and $V_{\frac{1}{2}}$ is the half-activation level; δ is the electrical distance across the membrane; and F/RT has its usual meaning.

If the number of channels in the open state a is n, and the total number of available channels at -70 mV is n_0, then the proportion of channels that are open is n/n_0. At the steady-state, $d(n/n_0)/dt = 0$, $n = n_\infty$, and

$$\frac{n_\infty}{n_0} = \frac{1}{1+\exp m V^* F/RT},$$

which is just the Boltzmann expression for the equilibrium distribution of gating charge in the membrane field. The linearized form of this expression is plotted in the inset of Fig. 4*B* and shows that the steady-state behaviour is consistent with the two-state gating model.

The linearized n_∞/n_0 *vs.* voltage relation from six fertilization experiments is shown in Fig. 5. The line was fitted to the experimental points using the method of least squares (linear correlation, 0·93). The slope of the relation was $-1{\cdot}7$, which gives the number of equivalent charges on the gating particle. $V_{\frac{1}{2}}$ determined from the zero intercept was -25 mV.

While there appears to be some scatter in the compiled data, the slope of the relation for each experiment is relatively constant. The scatter is restricted to movement of the relation along the voltage axis. Even within one experiment the relation shifted along the voltage axis in the positive direction at later times following insemination. This shift was usually not greater than 10–15 mV. A series resistance artifact could account for the direction of the shift. At high conductance with a large current flow part of the applied voltage drops across the series resistance. The true activation range for I_F is, therefore, less hyperpolarized than the applied voltage would indicate. As I_F decreases, the applied voltage would fall entirely across the membrane and the activation range for I_F would appear to shift towards less hyperpolarized potentials. However, typical voltage errors due to series resistance were 0·5–1·0 mV, which could not account for shifts in the activation potential of 10–15 mV.

A shift in the activation range for I_F could also be caused by a change in membrane surface potential resulting in a change in the absolute voltage difference across the membrane (Ohmori & Yoshii, 1978). This could be the result of any of a number of membrane processes occurring during fertilization – incorporation of charged sperm membrane components (Gabel, Eddy & Shapiro, 1979), exposure of charged egg membrane components during the cortical reaction, or changes in intracellular Ca – each of which could involve alterations of the membrane surface potential of the

egg in such a manner as to cause an apparent shift of the activation range of I_F along the voltage axis. For example, a decrease in intracellular calcium concentration would expose negative charges on the inner membrane and the true membrane voltage would be more hyperpolarized than expected from the applied voltage. Thus I_F would appear to activate at more positive potentials. Incorporation of negative charges on the inner membrane of the egg could cause a similar shift. It is interesting to note that parallel shifts were never seen for the activation of the Ca current (Fig. 3*C*), which suggests that localized changes in membrane surface potential might occur near fertilization channels.

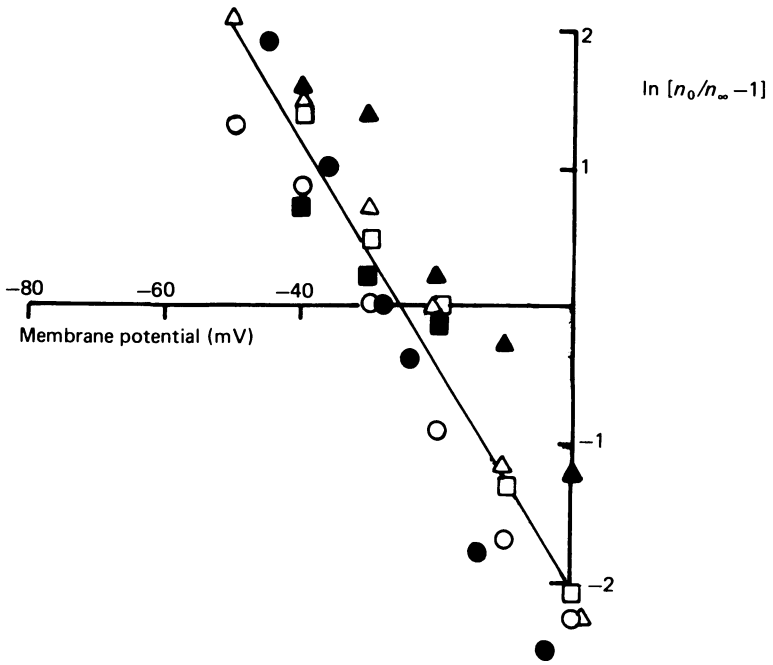

Fig. 5. The normalized steady-state conductance–voltage behaviour compiled for six different eggs. Details of the analysis are given in the text. Linear correlation was 0·93.

Kinetics

The two-state gating model makes a number of specific predictions about the time course of membrane current following step changes in potential. First, the time course of current should depend only on the voltage during the pulse. Secondly, the currents should relax without a lag along a single exponential time course. Finally, the relaxation time constant should be equal to the inverse of the sum of the rate constants, a condition which predicts that the time constant reaches a maximum value when the forward and reverse rate constants are equal. These predictions were tested in the experiments described below.

The time course of the tail current measured after repolarizing the membrane to −70 mV from various test potentials is shown in Fig. 6. The test potential (mV) is indicated at the side of each plot. The rate of the tail relaxation is independent of

the test potential amplitude. Its time course depends only upon the potential at which it is measured, in this case −70 mV, the repolarization potential.

In the next set of experiments the voltage dependence of the current relaxations was examined. When the membrane potential of the egg was held at −70 mV and then stepped to positive potentials, it was difficult to discern relaxations due to the

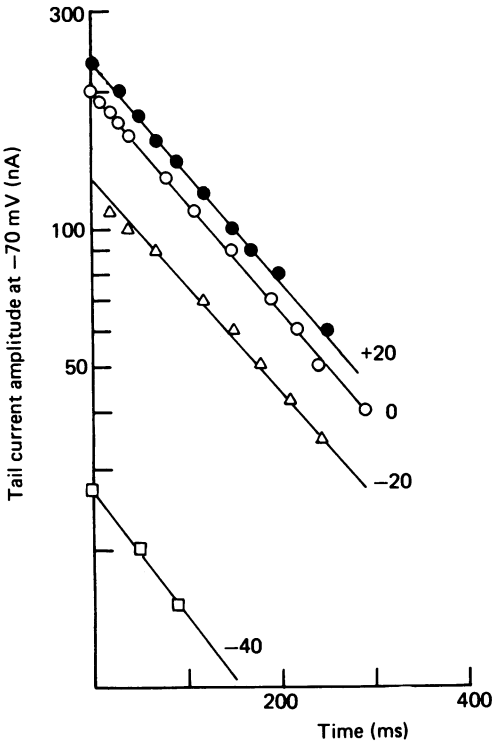

Fig. 6. Time course of the tail current relaxation following return of the membrane to the holding potential (−70 mV) after depolarizing voltage steps. The tail current amplitude was measured after repolarizing the cell to −70 mV from the test potentials (mV) indicated in the Figure. Lines drawn by eye.

time-dependent turn-off of I_F. This was because the driving force for ionic current flow diminished in the potential range where the channels were closing. The situation is illustrated in the experiment shown in Fig. 4*A*, where the Ca current relaxations were small relative to those due to I_F. Slight outwardly directed current relaxations during positive voltage steps can be seen in the current record. Note, however, how the amplitude of the relaxations decreased as the instantaneous current approached the zero current level (line above current record). The small amplitude of the current relaxations near the reversal potential made analysis of the current's time course difficult. In order to analyse the time course of the conductance change between −70 and 0 mV an alternative approach was adopted. The holding potential was shifted to 0 mV shortly after insemination when I_F reached its maximum steady level. The change in holding potential shifted the equilibrium such that a significant number

of channels were closed. Channels could be opened by stepping the membrane potential in the hyperpolarizing direction which produced a time-dependent inward current. Records from this experiment are shown in Fig. 7*A*. A semi-logarithmic plot of the normalized amplitude of the inward current against time is shown in Fig. 7*B* for several different test potentials. The current turns on with an exponential time course with a rate which increases with increasing hyperpolarization. In some cases

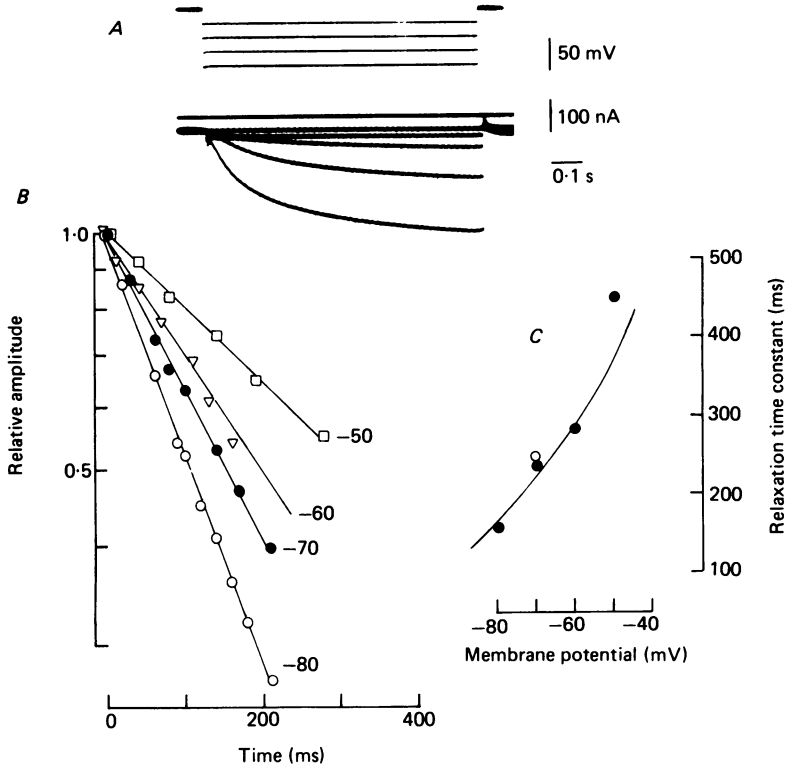

Fig. 7. *A*, time course of inward current elicited by hyperpolarizing voltage steps from a holding potential of 0 mV. Line above current record indicates the zero current level. The potential was shifted in 20 mV steps in the record. *B*, semilogarithmic plot of the normalized amplitude of the inward current against time after the onset of the pulse for several different test potentials (mV). *C*, the relaxation time constant as a function of membrane potential.

the current deviated from a single exponential at longer times. For potentials more negative than −80 mV, K current through anomalous rectifier channels contributed significantly to the total inward current (Hagiwara, Miyazaki & Rosenthal, 1976). Within the restricted potential range examined the current relaxations during hyperpolarization clearly became faster as the command potential became more negative. The relation between the relaxation time constant and voltage is illustrated in Fig. 7*C*. For comparison, the open circle in Fig. 7*C* is the tail current time constant measured after repolarizing the membrane to −70 mV, the resting potential, as described earlier. From these experiments it is concluded that the relaxation time constant is voltage-dependent, taking up a value appropriate to the potential at which it is measured.

To complete the study of the voltage-dependent current relaxations it was necessary to describe the time constant at positive membrane potentials. Voltage steps to positive potentials also activated outward current through delayed rectifier channels, making measurements of current relaxations uncontaminated by this K current impossible. The rate of the conductance relaxation could be directly observed,

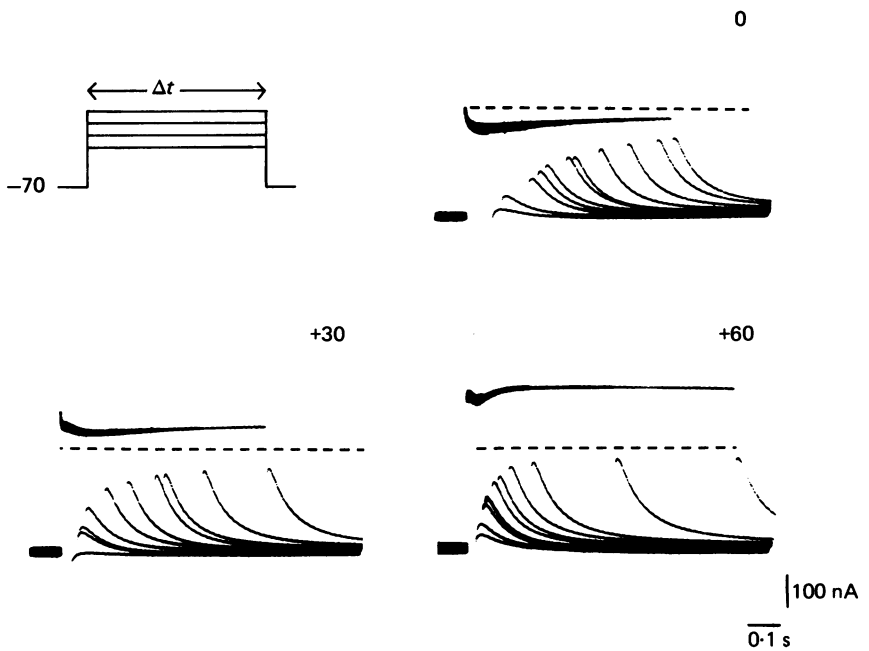

Fig. 8. Time course of the conductance decrease at positive membrane potentials. A cell was held at −70 mV and the potential stepped with pulses of increasing duration to the fixed values indicated in the Figure. Each record was made by superimposing the current response to pulses of varying duration on the oscilloscope. Dashed lines indicate the zero current level. The heavy trace is the current during the pulse, while the tail relaxations occur after the pulse is terminated. The envelope of the tail current amplitudes gives the time course of the conductance change.

however, by following the change in the initial amplitude of tail current (measured immediately after stepping the membrane potential back to the resting potential) as a function of pulse duration. An envelope experiment of this short is shown in Fig. 8. The holding potential of the egg was kept at −70 mV where the conductance was fully activated, and a depolarizing test potential of fixed amplitude but varying duration applied to the cell. Current traces were superimposed on the oscilloscope to give the records shown. The time course of deactivation can be seen as the envelope of the initial amplitudes of the superimposed tail currents (the dashed line in the Figure represents the zero current level; the voltage record is not shown). Fig. 8 shows that the tail current reached a final steady-state amplitude much more quickly as the command potential became more positive (compare 0 with +60 mV).

The value of the relaxation time constant was not determined from these records for the following reason. For short-duration test potentials (see for example the first tail current in the 0 and 30 mV records) the tail current showed a small, inward deflexion which became less prominent as the pulse

duration increased. The inward relaxation for short pulses was most probably due to an inward Ca current tail (see below). It became smaller with longer pulses due to voltage-dependent inactivation of the Ca permeability (Hagiwara *et al.* 1975; J. B. Lansman, unpublished observations). Therefore, determination of the actual amplitude of I_F tails for short pulses is inaccurate because of contamination by the inward Ca tail. Nevertheless it is clear that the relaxation time constant decreased with depolarization above 0 mV.

Analysis of the voltage-dependent current relaxations shows good agreement with first-order kinetics. The time constant depends on membrane potential and reaches a maximum value between −40 and 0 mV, a value consistent with the half-activation potential of −25 mV determined by steady-state analysis. Therefore, a two-state gating model provides an adequate description of the effect of voltage on the fertilization current.

Effect of external Ca

Application of the Ca ionophore A23187 is a sufficient stimulus for eliciting a fertilization potential in sea urchin eggs (Steinhardt & Epel, 1974; Chambers, Pressman & Rose, 1974). The mechanism of the permeability change responsible for the fertilization potential may therefore involve the binding of Ca to a site on the inner egg membrane. The source of this Ca appears to be intracellular (Steinhardt, Zucker & Schatten, 1977), yet there seems to be no information on whether Ca entry through action potential channels is involved in fertilization-specific permeability changes. Experiments described below examine the effects of Ca on I_F (Fig. 9).

An egg was fertilized under voltage clamp and I_F at the resting potential allowed to develop. The external solution was changed to ASW containing 50, 0 or 10 mM-Ca (Fig. 9*A*). The change in the steady inward current reflects the time course of the fertilization-specific conductance. In 50 mM-Ca ASW depolarizing voltage pulses produced a large inward Ca current superimposed on the currents flowing through the fertilization channels. This can be seen by comparing the records in 50 mM-Ca ASW with those obtained in 0 mM-Ca ASW In both 50 mM-Ca and 0 mM-Ca ASW the ohmic current jump at the beginning of the pulse and the tail current after the pulse are similar. In Fig. 9*B* the tail current amplitude as a function of time after the voltage step is plotted for the three Ca solutions. In Fig. 9*C* the fraction of channels open in the steady state as a function of voltage is plotted.

Two factors contributed to the inaccuracy of the analysis. An inwardly directed Ca tail current (compare 50 with 0 mM-Ca A.S.W.) obscured the initial amplitude of the tail relaxation. The initial amplitudes of the tail currents were, therefore, compared 50 ms after the termination of the voltage pulse. This was sufficient time for the Ca permeability to relax. Another difficulty was the initial inward surge of Ca current in 50 mM-Ca A.S.W. which made it difficult to determine the magnitude of the current immediately after the onset of the pulse.

Fig. 9*B* and *C* shows that both the steady-state voltage dependence and the kinetics of the tail relaxations are relatively insensitive to variations in extracellular Ca. However, it may be worth while examining this point at much higher Ca concentrations.

Ion selectivity

In ASW the reversal potential for I_F was $6{\cdot}0 \pm 5{\cdot}8$ mV (mean ± S.D., $n = 11$). The near-zero reversal potential of I_F suggests that the channel is not very selective and

that reversal potential is determined by the liquid junction potential between internal and external solutions. Reduction of the Cl concentration of the sea water to one tenth by replacement with methanesulphonate did not change either the magnitude of the inward current or its reversal potential, indicating that anions are negligibly permeant. External Ca was similarly without effect (see current records in Fig. 9), suggesting that divalent cations are also impermeant. Therefore, the selectivity is restricted to monovalent cations of which Na and K are the major permeant species in ASW.

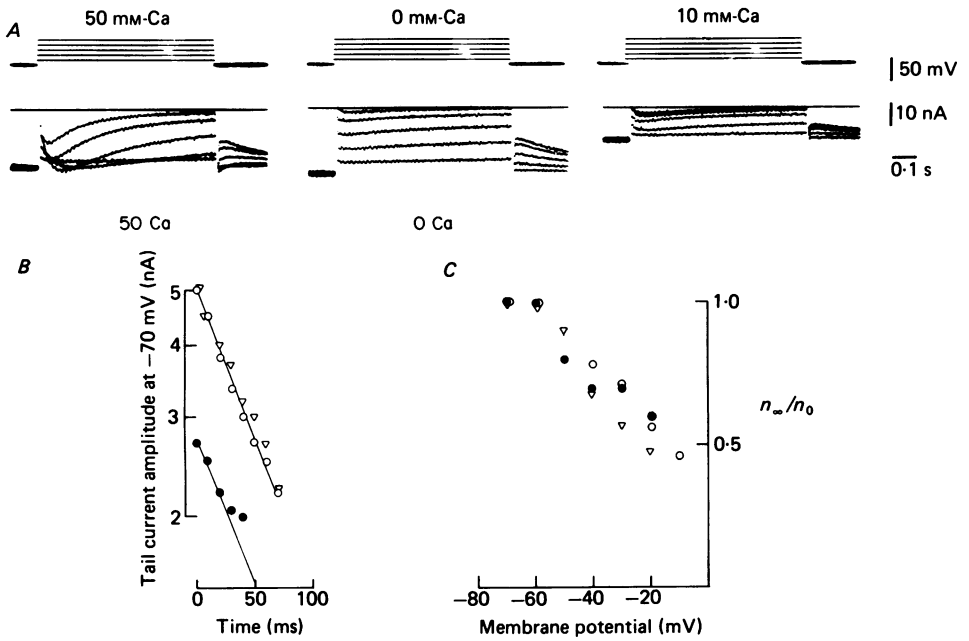

Fig. 9. The effect of extracellular Ca on the kinetics and steady-state voltage dependence of I_F. The Ca concentration was changed from normal (10 mM) to 50, 0 and 10 mM in order. Filled circles, 10 mM-Ca; open circles, 0 mM-Ca; open triangles, 50 mM-Ca. *A*, oscilloscope records. *B*, time course of the tail current following the end of the voltage pulse. *C*, voltage dependence of the fraction of open channels. Details in text.

Effect of Na

The effect of replacing Na with choline on the reversal potential of I_F is shown in Fig. 10. The top record (Fig. 10*A*) shows the time course of I_F as the Na concentration was varied. The reversal potential was determined from the reversal of the instantaneous current (Fig. 10*B*). Experimental groups were bracketed by controls in ASW. The results from five eggs are shown in Fig. 10*C*. The line drawn through the experimental points is the theoretical expectation for the change in reversal potential with changes in external Na as predicted by the constant field equation (Goldman, 1943; Hodgkin & Katz, 1949) with the assumption of voltage-independent permeability coefficients. It was calculated with intracellular K equal to 200 mM,

intracellular Na equal to 10 mM (Hagiwara & Yoshii, 1979), and assuming a ratio of Na and K permeabilities (P_{Na}/P_K) of 0·60. The results show that the channel does not discriminate greatly between Na and K. The effects of changes in K concentration were not studied because of the large influence of this ion on the resting K conductance (Hagiwara *et al.* 1976).

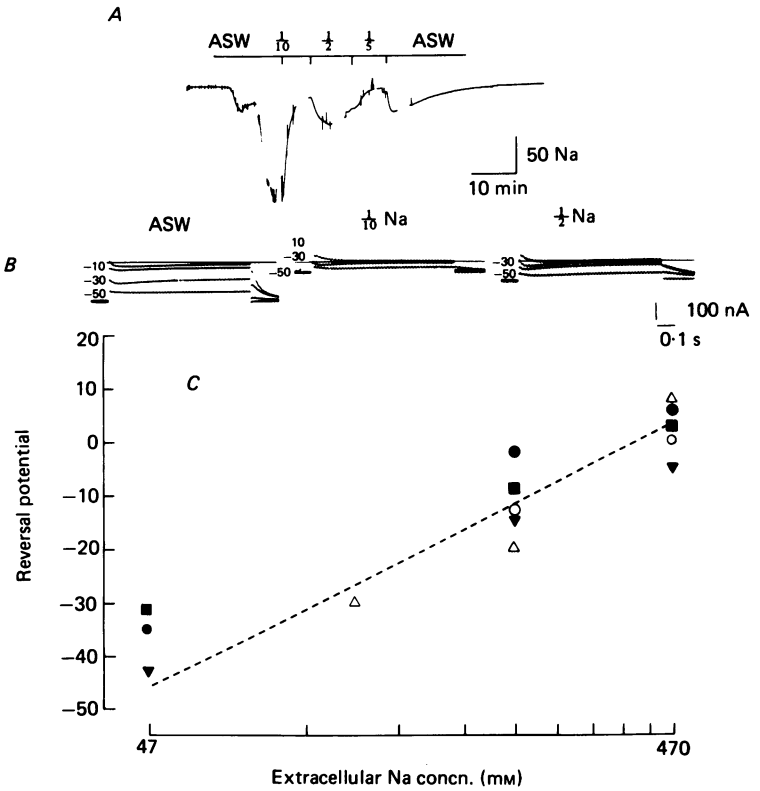

Fig. 10. Effect on the fertilization current of replacing extracellular Na with choline. *A*, chart record of the fertilization current showing the effects of lowering Na on the magnitude of the current. *B*, oscilloscope records of voltage-clamp currents in low-Na A.S.W. Line in current record indicates zero current level. *C*, dependence of the reversal potential of I_F on extracellular Na. Each symbol represents data from a different egg. Line represents the theoretical expectation from the constant field equation with $P_{Na}/P_K = 0{\cdot}60$.

Effects of Li, Cs and Rb

The effects of Li, Cs and Rb were tested in three cells. The Na in ASW was replaced completely with one of these cations and the reversal potential of I_F determined as shown in Fig. 11 for one egg. The average reversal potential in Li ASW was $-19{\cdot}7 \pm 8{\cdot}1$ mV, in Cs ASW $+9{\cdot}3 \pm 5{\cdot}5$ mV, and in Rb ASW $+25{\cdot}8 \pm 5{\cdot}6$ mV. Permeability ratios were determined using the following form of the GHK equation:

$$V_0 = \frac{RT}{F} \ln \frac{P_X/P_K [X]_o + [K]_o}{P_{Na}/P_K [Na]_i + [K]_i},$$

where square brackets denote concentration, subscripts 'i' and 'o' represent intracellular and extracellular respectively, and where $[X]_o$ = 470 mM-Li, -Cs or -Rb. Comparison of the relative permeability P_X/P_K yielded the sequence Rb > K > Cs,Na > Li with ratios 1·2:1·0:0·6:0·6:0·2.

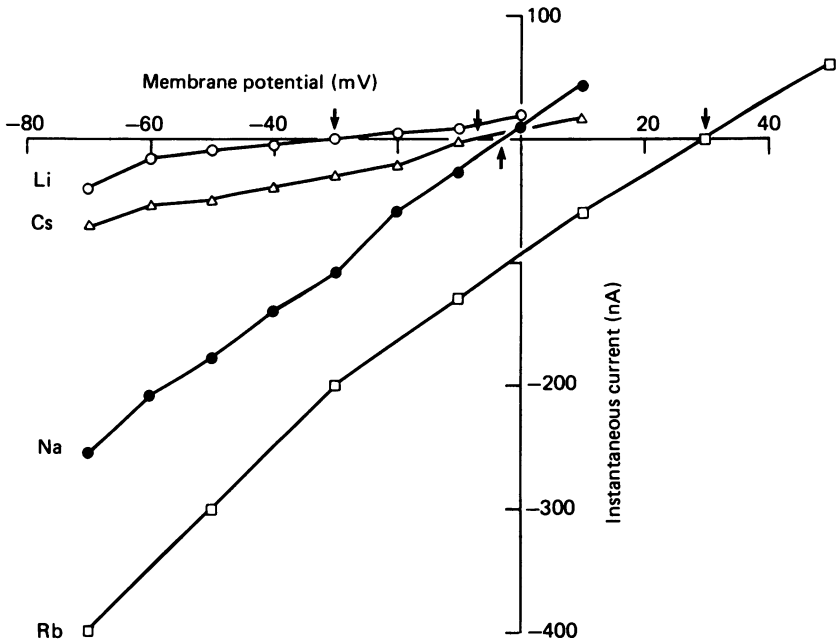

Fig. 11. Instantaneous current–voltage relations measured in ASW in which Na was replaced with Cs, Li or Rb. Measurements made in a single egg. The reversal potential is indicated with an arrow.

DISCUSSION

This paper reports a voltage-clamp study of the fertilization potential of a starfish egg. The currents activated by sperm were found to be the result of a time-dependent change in membrane permeability to monovalent cations. The fertilization current, I_F, activated and inactivated over a time course of several tens of minutes. Membrane potential has two effects on I_F: one on the over-all time course of the permeability change, the other on the equilibrium distribution of open channels. The nature of the fertilization-induced conductance and its relation to cellular and membrane events occurring during fertilization are considered below.

Nature of the permeability change

The present results demonstrate that the time course of I_F is adequately explained as a time-dependent change in membrane conductance. Fertilization induces a large increase in chord conductance at the resting level and the decline of the current was due to a decrease in conductance towards the pre-fertilization levels. Neither the development of an outward counter-current nor a time-dependent change in reversal potential could account for the time course of I_F.

How sperm trigger a change in the permeability of the egg membrane is not known. The ability of 'parthenogenic' substances to activate eggs (Loeb, 1913) and to induce fertilization potentials (Steinhardt & Epel, 1974; Jaffe *et al.* 1979) in the absence of sperm suggests that the structures mediating the change in permeability are constituents of the egg membrane. The similarity of the fertilization potential triggered by sperm and the activation potential triggered artificially implies that they act through a common step such as a second messenger.

One hypothesis is that intracellular Ca fulfils such a second messenger role. According to this hypothesis, the time course of I_F would reflect the time-dependent change in the intracellular Ca concentration, $[Ca]_i$. Several lines of evidence suggest that Ca ions do, in fact, play such a role. In the sea urchin egg the Ca ionophore A23187 (Steinhardt & Epel, 1974) is able to initiate the fertilization potential. In the frog egg, where membrane depolarization during fertilization is due to Cl efflux, injection of Ca but not Mg into an egg through a micropipette (Cross, 1981), or exposure to Ca ionophore (Schlichter & Elinson, 1981), are both equally sufficient stimuli for inducing the potential change. The ability of $[Ca]_i$ to regulate an inward current in an egg was demonstrated during internal perfusion of the tunicate egg with Ca-containing solutions. These experiments showed a time-dependent change in holding current under voltage clamp when $[Ca]_i$ was raised from 0 to approximately 10^{-5} M (Takahashi & Yoshii, 1978), an effect due presumably to egg activation by increased $[Ca]_i$.

If the Ca hypothesis is correct, the change in the egg permeability might occur through the activation of a Ca-dependent ion channel much as Ca acts to turn on K current (see Meech, 1978) or non-specific cation current (Kass, Lederer, Tsien & Weingart, 1978*a*; Kass, Tsien & Weingart, 1978*b*; Colquohoun, Neher, Reuter & Stevens, 1981) in other preparations. Although the fertilization channels show low selectivity for Na over K, the small permeability of Li relative to Na or K and the strong voltage sensitivity are properties not shared with the Ca-activated non-selective cation channels which have been reported in the literature (Colquhoun *et al.* 1981).

Voltage-dependent gating

In this study, fast and slow voltage-dependent gating kinetics were identified. First, the decay of I_F was more rapid when the holding potential was set more positive than rest. Secondly, at any time during I_F, step changes in membrane potential could shift the fraction of channels that were open to a new equilibrium value. Voltage, therefore, exerts its action on two separate kinetic processes corresponding to different steps in the reaction generating I_F. Voltage dependence of the currents could arise if any step from attachment of sperm to the subsequent permeability change has voltage-dependent rate constants. For example, attachment, fusion, or incorporation of the sperm membrane could in principle be regulated by the voltage across the membrane. Voltage could also influence processes regulating $[Ca]_i$ such as release or uptake by intracellular stores and regulation across the cell membrane. The experimental results do not distinguish between these possibilities. Nonetheless, a useful working model may be proposed which assumes that the effect of voltage on the decay of I_F may be due to an effect of voltage on either the availability of intracellular Ca or, alternatively, the binding of Ca to a site on the channel. The fast

voltage-dependent kinetics presumably arise from an inherent voltage sensitivity of the open channel which controls the equilibrium distribution of closed and open channels at any fixed level of $[Ca]_i$. Many more experiments will be required before the mechanism of the permeability change is understood in any detail.

Physiological significance

There is good evidence suggesting that one function of the fertilization potential in the echinoderm egg is to prevent polyspermic fertilization by blocking the fusion of extra sperm to the egg membrane (Jaffe, 1976; Miyazaki & Hirai, 1979). The efficiency of such a block to polyspermy would depend on how fast the membrane could depolarize to the blocking potential. The net effect of the voltage sensitivity of I_F is to produce a time-dependent rectification. During membrane depolarization, as, for example, during action potential generation following sperm attachment, the rectifying properties of I_F would act to keep total membrane conductance low. The action potential would be generated against a potential-dependent decline of the conductance due to fertilization. At positive membrane potentials this would prevent shunting of the peak of the action potential and ensure a rapid rate of rise following the first successful sperm entry.

This work was done in the laboratory of Professor S. Hagiwara whose advice and support I am happy to acknowledge. In addition I thank Drs M. Barish, W. Moody and H. Ohmori for helpful discussions. The work was supported by NIH grant NS 09012 to S. Hagiwara and MHTP training grant MH 15345.

REFERENCES

CHAMBERS, E. L. & DIARMENDI, J. (1979). Membrane potential, action potential and activation potential of eggs of the sea urchin, *Lytechinus variegatus*. *Expl Cell Res.* **122**, 203–218.

CHAMBERS, E. L., PRESSMAN, B. C. & ROSE, B. (1974). The activation of the sea urchin egg by the divalent ionophores A23187 and X537A. *Biochem. biophys. Res. Commun.* **60**, 126–132.

COLQUHOUN, D., NEHER, E., REUTER, H. & STEVENS, C. F. (1981). Inward current channels activated by intracellular Ca in cultured cardiac cells. *Nature, Lond.* **294**, 752–754.

CROSS, N. L. (1981). Initiation of the activation potential by an increase in intracellular calcium in eggs of the frog, *Rana pipiens*. *Devl Biol.* **85**, 380–384.

GABEL, C. A., EDDY, E. M. & SHAPIRO, B. M. (1979). After fertilization, sperm surface components remain as a patch in sea urchin and mouse embryos. *Cell* **18**, 207–215.

GOLDMAN, D. E. (1943). Potential, impedance, and rectification in membranes. *J. gen. Physiol.* **27**, 37–60.

HAGIWARA, S. & JAFFE, L. A. (1979). Electrical properties of egg cell membranes. *A. Rev. Biophys. Bioengng.* **8**, 385–416.

HAGIWARA, S., MIYAZAKI, S. & ROSENTHAL, N. P. (1976). Potassium current and the effect of Cs on this current during anomalous rectification of the egg cell membrane of a starfish. *J. gen. Physiol.* **67**, 621–638.

HAGIWARA, S., OZAWA, S. & SAND, O. (1975). Voltage clamp analysis of two inward current mechanisms in the egg cell membrane of a starfish. *J. gen. Physiol.* **65**, 617–644.

HAGIWARA, S. & YOSHII, M. (1979). The effects of internal potassium and sodium on the anomalous rectification of the starfish egg as examined by internal perfusion. *J. Physiol.* **292**, 251–265.

HIRAMOTO, Y. (1959). Electric properties of echinoderm eggs. *Embryologia* **4**, 219–235.

HODGKIN, A. L. & KATZ, B. (1949). The effect of sodium ions on the electrical activity of the giant axon of the squid. *J. Physiol.* **108**, 37–77.

IKEGAMI, S. (1976). Role of asterosaponin A in starfish spawning induced by gonad-stimulating substance and 1-methyladenine. *J. exp. Zool.* **198**, 359–366.

ITO, S. & YOSHIOKA, K. (1973). Effects of various ionic compositions upon the membrane potentials during activation in sea urchin eggs. *Expl Cell Res.* **78**, 191–200.

JAFFE, L. A. (1976). Fast block to polyspermy in sea urchin eggs is electrically mediated. *Nature, Lond.* **261**, 68–71.

JAFFE, L. A., GOULD-SOMERO, M. & HOLLAND, L. (1979). Ionic mechanism of the fertilization potential of the marine worm, *Urechis caupo* (Echiura). *J. gen. Physiol.* **73**, 469–492.

KANATANI, H. (1973). Maturation-inducing substances in starfishes. *Int. Rev. Cytol.* **35**, 253–298.

KASS, R. S., TSIEN, R. W. & WEINGART, R. (1978*b*). Ionic basis of transient inward current induced transient inward currents and aftercontractions induced by strophanthidin in cardiac Purkinje fibres. *J. Physiol.* **281**, 187–208.

KASS, R. S., TSIEN, R. W. & WEINGART, R. (1978*b*). Ionic basis of transient inward current induced by strophanthidin in cardiac Purkinje fibres. *J. Physiol.* **281**, 209–226.

LOEB, J. (1913). *Artificial Parthenogenesis and Fertilization.* University of Chicago Press.

MCCLENDON, J. F. (1910). Electrolytic experiments showing an increase in permeability of the egg to ions at the beginning of development. *Science, N.Y.* **32**, 122–124.

MEECH, R. W. (1978). Calcium-dependent potassium activation in nervous tissues. *A. Rev. Biophys. Bioeng.* **7**, 1–18.

MIYAZAKI, S. (1979). Fast polyspermy block and activation potential: electrophysiological bases for their changes during maturation of a starfish. *Devl Biol.* **70**, 341–354.

MIYAZAKI, S. & HIRAI, S. (1979). Fast polyspermy block and activation potential: correlated changes during ooctye maturation of a starfish. *Devl Biol.* **70**, 327–340.

MIYAZAKI, S., OHMORI, H. & SASAKI, S. (1975*a*). Action potential and non-linear current–voltage relation in starfish oocytes. *J. Physiol.* **246**, 37–54.

MIYAZAKI, S., OHMORI, H. & SASAKI, S. (1975*b*). Potassium rectifications of the starfish oocyte membrane and their changes during oocyte maturation. *J. Physiol.* **246**, 55–78.

MOODY, W. J. & LANSMAN, J. B. (1983). Development regulation of Ca and K currents during hormone-induced maturation of starfish oocytes. *Proc. natn. Acad. Sci. U.S.A.* **80**, 3096–3100.

OHMORI, H. & YOSHII, M. (1977). Surface potential reflected in both gating and permeation mechanisms of sodium and calcium channels of the tunicate egg cell membrane. *J. Physiol.* **267**, 429–463.

SCHLICHTER, L. C. & ELINSON, R. P. (1981). Electrical responses of immature and mature *Rana pipiens* oocytes to sperm and other activating stimuli. *Devl Biol.* **83**, 33–41.

SHEN, S. & STEINHARDT, R. A. (1976). An electrophysiological study of the membrane properties of the immature and mature oocyte of the Batstar, *Patiria miniata. Devl Biol.* **48**, 148–162.

STEINHARDT, R. A. & EPEL, D. (1974). Activation of sea urchin eggs by a calcium ionophore. *Proc. natn. Acad. Sci. U.S.A.* **71**, 1915–1919.

STEINHARDT, R. A., LUNDIN, L. & MAZIA, D. (1971). Bioelectric responses of the echinoderm egg to fertilization. *Proc. natn. Acad. Sci. U.S.A.* **68**, 2426–2430.

STEINHARDT, R., ZUCKER, R. & SCHATTEN, G. (1977). Intracellular calcium release at fertilization in the sea urchin egg. *Devl Biol.* **58**, 185–196.

TAKAHASHI, K. & YOSHII, M. (1978). Effects of internal free calcium upon the sodium and calcium channels in the tunicate egg analysed by the internal perfusion technique. *J. Physiol.* **279**, 519–549.

TYLER, A., MONROY, A., KAO, C. Y. & GRUNDFEST, H. (1956). Membrane potential and resistance of the starfish egg before and after fertilization. *Biol. Bull.* **111**, 153–177.